



Article

Coexistence of a Marginal Mountain Community with Large-Scale and Low Kinematic Landslide: The Intensive Monitoring Approach

Danilo Godone ¹, Paolo Allasia ^{1,*}, Davide Notti ¹, Marco Baldo ¹, Flavio Poggi ² and Francesco Faccini ^{1,3}

- ¹ Istituto di Ricerca per la Protezione Idrogeologica, Consiglio Nazionale delle Ricerche, 10135 Torino, Italy; danilo.godone@irpi.cnr.it (D.G.); davide.notti@irpi.cnr.it (D.N.); marco.baldo@irpi.cnr.it (M.B.); faccini@unige.it (F.F.)
- ² Dipartimento Ambiente e Protezione Civile, Settore Interventi Difesa del Suolo, Regione Liguria, 16146 Genova, Italy; flavio.poggi@regione.liguria.it
- ³ Dipartimento di Scienze della Terra, dell'Ambiente e della Vita, Università degli Studi di Genova, 16132 Genova, Italy
- * Correspondence: paolo.allasia@irpi.cnr.it

Abstract: Mountain territories affected by natural hazards are vulnerable areas for settlements and inhabitants. Additionally, those areas are characterized by socio-economic marginality, further favoring their abandonment. The study area is located in Liguria (Italy), and a large, slow-moving phenomenon endangers the settlements in the region. Monitoring such phenomena requires the use of instruments capable of detecting yearly, millimetric displacements and, due to their size, the use of remote techniques which can provide deformation measurement of the entire extent of the phenomenon. The methodology proposed here couples long-term interferometric remote sensing data analysis with intensive in situ monitoring (inclinometer, piezometers and global navigation satellite systems). Furthermore, the inclinometric measurements were carried out with an experimental, robotized inclinometer. The aim is to frame the overall context of ground deformation, assure information for inhabitants, stakeholders and land-planners, and secure coexistence with the phenomenon. Remote sensing provided a time series of 28 years of deformation measurements while in situ instrumentations allowed, in the last years, a better understanding of the surficial and deep behavior of the phenomenon, confirming the satellite data. Additionally, the high-frequency monitoring allowed us to record acceleration after precipitation peaks. The proposed approach, including the experimental instruments, proved its viability and can be replicated in similar mountain contexts.

Keywords: slope monitoring; marginal territories; senior citizens; mountain areas depopulation



Citation: Godone, D.; Allasia, P.; Notti, D.; Baldo, M.; Poggi, F.; Faccini, F. Coexistence of a Marginal Mountain Community with Large-Scale and Low Kinematic Landslide: The Intensive Monitoring Approach. *Remote Sens.* **2023**, *15*, 3238. <https://doi.org/10.3390/rs15133238>

Academic Editors: Renato Macciotta, Lu Zhuo and F. Albert Liu

Received: 31 March 2023

Revised: 20 June 2023

Accepted: 20 June 2023

Published: 23 June 2023



Copyright: © 2023 by the authors. Licensee MDPI, Basel, Switzerland. This article is an open access article distributed under the terms and conditions of the Creative Commons Attribution (CC BY) license (<https://creativecommons.org/licenses/by/4.0/>).

1. Introduction

From the beginning of civilization, human settlements have had to cope with interactions involved with slope instabilities. Various solutions to the issue have been tried; e.g., phenomena monitoring can improve the coexistence of the population along with other risk-mitigation strategies like maintenance, in particular of large, very slow landslides [1], which allow the persistence of the settlement over time. Inhabitant relocation is considered a last resort due to social and economic reasons, and the last resort is rarely applied except after the occurrence of paroxysmal events. Since the Roman age, residents of landslide-affected areas have struggled to mitigate the effects of landslides while occupying the same territory [2]. In more recent times, such as the Middle Ages, landslide impacts were described and documented [3], and in the modern era, these events have been monitored with measuring systems [3]. Currently, the scenario is complicated by the increasing depopulation [4,5], the aging of mountain settlements, inhabitants and their vulnerability [6], and the growing marginality of those areas [7]. In Italy, 53% of the municipalities are

classified as mountain territories according to Laws 991/1952 and 657/1957 (Figure 1). A specific commission monitors the inclusion of municipalities in that list and defines “partially mountainous municipalities” as those who fulfill the requisites mentioned above in only a fraction of their territories. In these areas, there are approximately 5.1 million senior citizens (i.e., older than 65), representing 8.64% of the overall Italian population according to National Census Data (ISTAT—www.istat.it (accessed on 30 March 2022)). Additionally, there is a prevalence of subjects over the age of 74, highlighting a relevant vulnerability and the risk of social exclusion [8]. The marginality is computed by several social and economic parameters and synthesized in indexes [9,10] by various governmental agencies (e.g., Agenzia per la Coesione Territoriale—Agency for Territorial Cohesion—www.agenziacoesione.gov.it (accessed on 30 March 2022)), such as the IVSM (Indice di Vulnerabilità Sociale e Materiale—Index of Social and Material Vulnerability) [9]. Territories with a high degree of vulnerability deserve special attention regarding interventions, planning and public services. Considering these social issues, an accurate and updated monitoring approach can provide land-planning managers, stakeholders and inhabitants with data and information, codified to increase their understanding based on the targets’ level of expertise [11], allowing them to cope and adequately coexist with the phenomenon and to take the necessary actions in response to the acquired data.

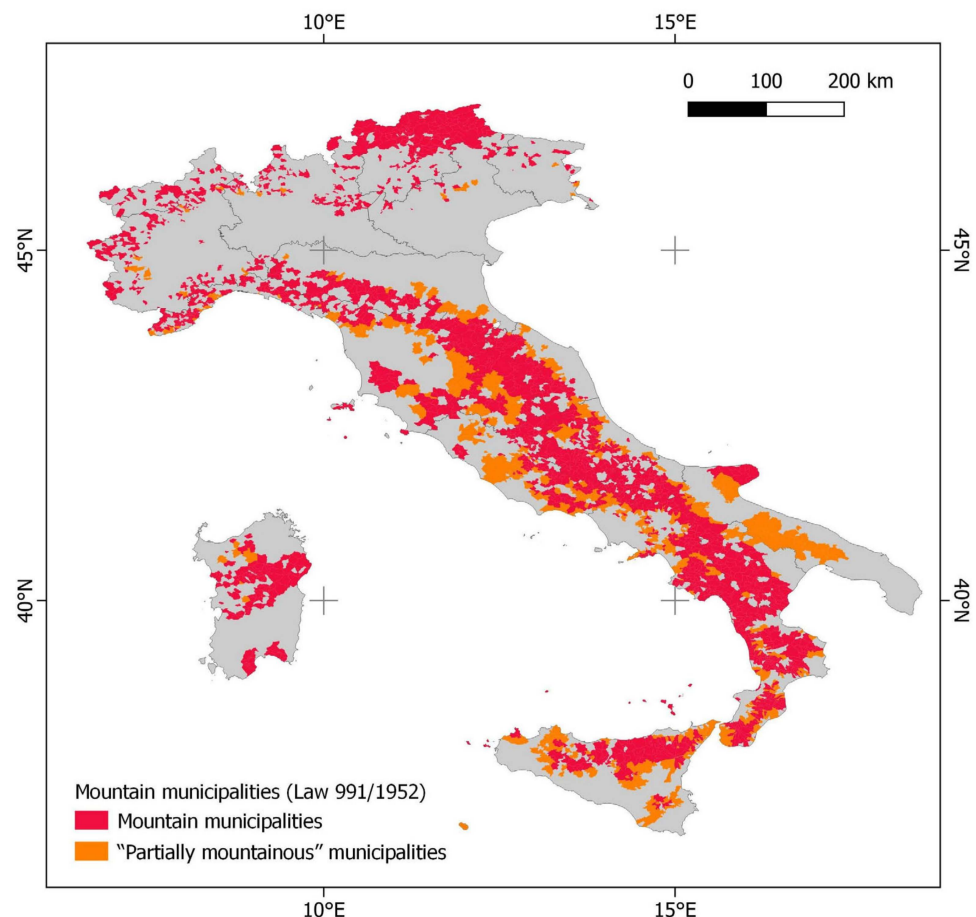


Figure 1. Mountain municipalities featuring medium to high socio-economic marginality (IVSM > 98) in Italy.

Landslides in the Mediterranean region are extremely widespread slope processes, varying in size from small slope failures to collapses that affect the entire ridge–slope–valley system. Landslides are classified according to causal factors, type of geomaterial, landslide scale, type of movement or triggering mechanisms [12]. A landslide greater than 10^5 m² and with a volume greater than 10^6 m³ is generally accepted as a large-scale landslide.

Large-scale landslides are characterized by generally complex failure mechanisms and are controlled by the geological and tectonic setting of the region [13,14]. Ground conditions such as adversely oriented structural discontinuities or contrasts in permeability and its effects on groundwater contrast in stiffness, geomorphological processes such as tectonic uplift, fluvial erosion of slope toe and physical processes such as rainfall and earthquakes are among the most frequent landslides factors [14,15]. Since historical times, large-scale landslides have been chosen as preferred sites for settlements and infrastructures, due to the low steepness of the area and the availability of groundwater and workable soil for agricultural purposes [16]. Large slope deformations, although featuring slow to extremely slow velocities, are characterized by a long-term evolution [13,17–19]. Their continuous displacement rates can put human settlements at risk not only for catastrophic evolution but also in terms of the ordinary use of infrastructures and buildings [20–22]. Additionally, these phenomena may cause the activation of secondary landslides, increasing the hazard level and complicating the comprehension of the whole phenomenon, which causes difficulties in terms of monitoring and planning mitigation actions [23].

The type of observed slope deformation, its kinematics and potential evolution can eventually define the need for an early warning system [24–27]. Several approaches have been proposed and carried out to monitor such kinds of phenomena. Among the most used are remote sensing techniques and terrestrial (in situ) systems, the latter using geomatics or geotechnical methodologies [28]. Their integrated use in a multidisciplinary combination is recommended for more effective and accurate action [29]. Remote sensing systems are based on displacement sensing by spaceborne SAR techniques, which allows cost-effective monitoring of large areas [30,31] and assessment of damage to infrastructure [32]. A drawback to remote sensing is the influence of the slope's geographical orientation and vegetation cover, which can hinder the reliability of the measurement or even its execution [33].

On the other hand, optical and multispectral remote sensing can be used to recognize the behavior of secondary landslides related to the main phenomenon; even with UAV-mounted sensors or aerial platforms [18,21]. Additionally, by exploiting the capabilities of structure from motion (SfM) algorithms, acquired imagery can be post-processed into three-dimensional models that, if acquired repeatedly, can provide insights into landslide dynamics [34]. A similar result can be obtained, even under tree cover, by a time series of airborne LiDAR surveys [35]. In situ measurements can provide timely information concerning slope deformation behavior. Repeated surveys can be completed by GNSS or robotized total stations [36–38] or by using IoT boards and sensors placed at key points on the landslide. After a series of campaigns, the approach supplies a series of vectors describing the landslide activity. Concerning geotechnical monitoring, several instruments, such as tiltmeters or extensometers, can be deployed to obtain a punctual measurement of the tilt and deformation of a particular feature. Importantly, inclinometers and piezometers can be used to carry out subsurface monitoring [39].

Furthermore, to achieve high-frequency data, it is possible to use automated inclinometers [40]. It is essential to carefully plan the acquisition strategy (e.g., instrumentation type, accuracy, resolution and measurement frequency) to adequately describe the phenomenon. Moreover, coupling surface and subsurface approaches can further improve detection of the parameters relevant to the deformation evolution [25,27].

To frame the overall context, this research describes the social issues and geologic features of a mountain slope in the Ligurian Apennines (Northwestern Italy). Two monitoring approaches were carried out to comprehensively assess the landslide dynamics: (i) a time series of historical to recent remote sensing data was compiled which, in the last years, involved (ii) multidisciplinary, high frequency, in situ monitoring. Results from the above-mentioned methodologies confirmed the deformation trend. They provided meaningful information concerning the landslide that was shared with the regional and municipal administration and the local population to ensure the best coexistence strategy for the future, with a view to the sustainable development of those mountain areas.

2. Materials and Methods

2.1. Study Area

2.1.1. Geomorphological Settings

Liguria is one of the Italian regions with the highest percentage of the population living in landslide-prone areas: nearly 900,000 inhabitants, or 54.9% of the total population. Almost 6% of the people live in high or very high landslide-hazard areas, which is the highest in the nation [41]. Liguria, out of a total area of 5416 km², encompasses more than 100 km² of very high landslide-hazard and almost 700 km² of high hazard areas. Due to its physical–geographical, geological and geomorphological features, nearly 60% of the whole territory is mapped as having a risk of significant hazard. The area is historically characterized by a high quantity of geo-hydrological events and, consequently, damage and fatalities [42–45]. Among the various Ligurian Tyrrhenian basins, the Entella Stream catchment (Figure 2a,b), in addition to being one of the largest, is also among those most representative of different geohydrological processes, such as shallow landslide events [46], and contains villages historically built on ancient and relict, but often reactivated, deep-seated, large-scale landslides. Within the three sub-basins of the Entella Stream, the Graveglia Stream catchment is probably the best known, not only because of its mining history related to its numerous manganese and sulfide mines but also because of its geological and geomorphological setting.

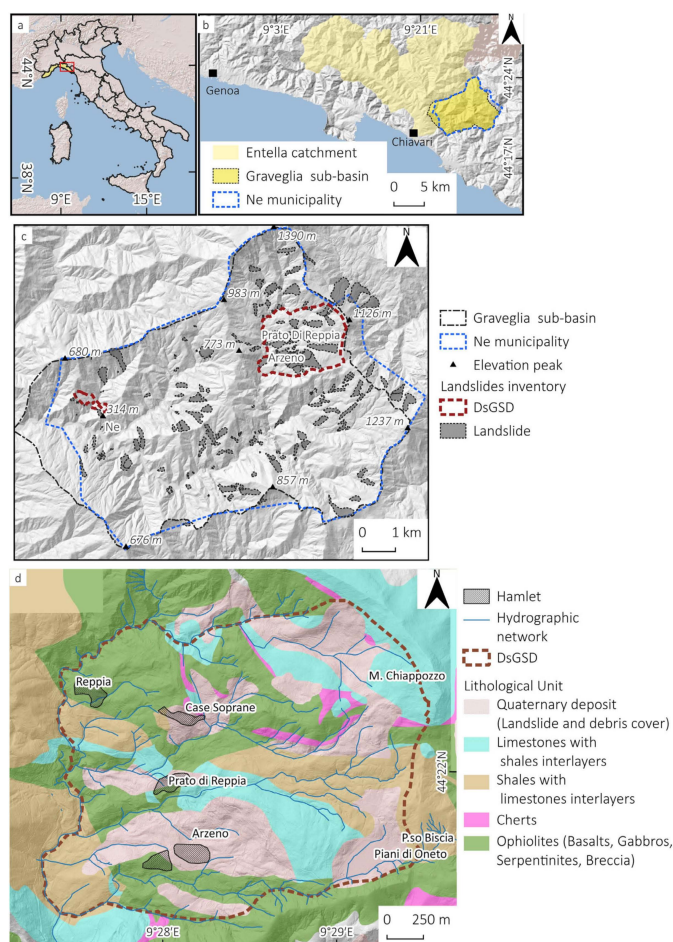


Figure 2. (a) Location of Liguria region (yellow and study area, red box); (b) The Graveglia valley inside the Entella basin; (c) Landslide inventory map (derived from [47], available on Regione Liguria cartographic service (WFS) of the Graveglia Basin and affected hamlets locations. DsGSD boundary plotted from the investigations reported in [48]); (d) Lithological map of the study area derived from 1:50,000 geological map “Sestri Levante” of CARG project [49,50], download from Regione Liguria cartographic service (WFS).

The study area is located in upper Graveglia Valley (Figure 2b), in the municipality of Ne (Metropolitan City of Genova). The geological setting is quite complex: the outcropping of bedrock formations in the study area belong to the Bracco-Val Graveglia Unit. They are composed of a Jurassic ophiolitic sequence (serpentinites, gabbros, basalts and associated ophiolitic breccias) overlaid by a Jurassic–Cretaceous deep-sea sedimentary sequence comprising cherts, limestones and shales [51]. The geological setting is one of the landslide-predisposing factors for the large deformation affecting upper Graveglia Valley. Among the several large-scale landslides in the upper Graveglia Valley [48,52,53], this research addresses the deep-seated gravitational slope deformation (DsGSD) that involves the entire slope from the Mt. Chiappozzo ridge to the valley floor, affecting the hamlets of Reppia, Prato di Reppia (PDR) and Arzeno (ARZ), and including Piani di Oneto (PDO), interpreted as complex DSGSD trench and subordinately karst depression (Figure 2c). There are several morphological indicators, such as (a) the large closed depressions of the Pian di Oneto and Casoni di Chiappozzo, located in the upper slope and related to trenches; (b) the doubling of the ridge; (c) several anomalies in the hydrographic network, with river elbows, confluences against the flow and even the displacement of parts of watercourses; (d) large areas of highly fractured and altered rock mass associated with the geological layout (with the less resistant and more deformable shales at the base and the more rigid ophiolite masses above); and (e) several huge landslide bodies, suggesting extensive deep-slope gravitation deformation limited to the east by Monte Chiappozzo and the west by the riverbed of Reppia torrent. The DsGSD shows several sub-sectors and secondary active landslides (Figure 2b), already mapped in the IFFI inventory, with more active deformations that have caused widespread damage, especially to the ARZ and PDR hamlets. The prolonged action of the phenomenon is visible, for instance, in disconnected and fractured roads (Figure 3a), even though the municipal authorities have repeatedly carried out pavement repairs. Another indirect kinematic indicator is the presence of many fractures on the walls of several buildings (Figure 2b–d). The damage ranges from slight to moderate, especially on old buildings without maintenance. According to the ISTAT database (<https://www.istat.it/it/mappa-rischi/indicatori> (accessed on 9 March 2023)), most of the buildings (86%) were built before 1980 and are made by masonry (90%).

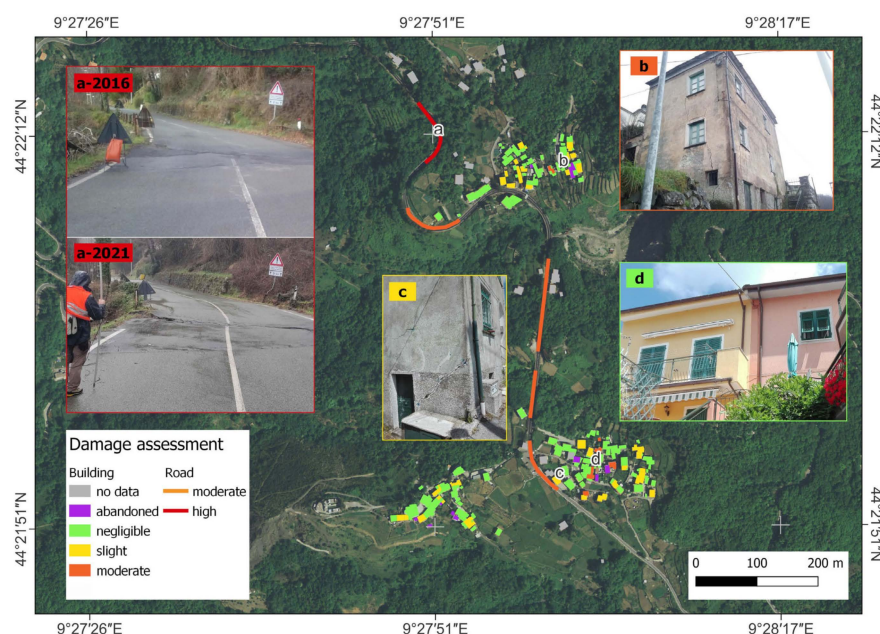


Figure 3. Damage assessment in the study area. (a) Road cracks and displacements in 2016 and 2021; (b) moderate damage on an abandoned building in PDR; (c) slight damage on an old building in ARZ; (d) negligible to slight damage in a recent maintained building in ARZ.

2.1.2. Socio-Economic Setting

The area features a high presence of senior citizens, i.e., approximately 50% of the inhabitants of both hamlets; moreover, the entire municipality is split into 30 hamlets beyond the main settlement, causing a considerable number of inhabitants (46.89%) to commute daily inside and outside municipal boundaries. Therefore, the inhabitants are severely exposed to geo-hydrological risks. Additionally, due to the reduction of mining activity in the valley, the number of inhabitants is continuously decreasing, with a drop of 60% in the last 160 years according to Ne municipal records. According to IVSM, the municipality is classified as medium to highly vulnerable (99.08 score) to the risks of uncertain conditions and is susceptible to result in factual economic/social discomfort.

2.2. Monitoring Strategies

2.2.1. InSAR Monitoring

Before 2018, the only available data regarding landslide displacement was through InSAR satellite analysis (Table 1). Due to the slope having a gentle orientation to the west and the widespread presence of anthropic structures and talus, the Arzeno landslides are particularly suitable for persistent-scatter InSAR analysis (MT-InSAR). Approximately 28 years of MT-InSAR data are available from different satellites, starting with ERS1/2 (1992–2000) and then followed by ENVISAT (2003–2011), Cosmo-SkyMed (2011–2014) and Sentinel-1 (2015–2020). The previously processed data from ERS, ENVISAT and Cosmo-SkyMed were downloaded from the “Piano Straordinario di Telerilevamento Ambientale” database (PST) [54], carried out by the Italian Ministry of Environment. These datasets were processed using PSInSARTM [55] and SqueeSARTM algorithms [56] by TRE-Altamira and E-Geos.

Table 1. Technical features of InSAR datasets.

Satellite	Source	Processing	From	To	Geometry	Inc. Angle (Approx)
ERS1/2	PST	PSInSAR TM	6 July 1992	30 November 2000	Ascending and Descending	23°
ENVISAT	PST	PSInSAR TM	8 April 2003	15 June 2010		23°
CSKM	PST	SqueeSAR TM	7 July 2011	25 March 2014		34°
Sentinel-1	Liguria Region	SqueeSAR TM	22 March 2015	8 December 2019		41°
Sentinel-1 (EGMS)	EGMS	Various	22 March 2015	30 June 2020		41°

Regione Liguria kindly provided Sentinel-1 data (2015–2019) processed with SqueeSARTM algorithm by TRE-Altamira. We also used the Sentinel-1 data (2015–2020), available through the European Ground Motion Service (EGMS). The EGMS [57–59] is an open-source service, part of the Copernicus Land Monitoring Service, that provides previously processed (by several companies and algorithms [59]) MT-InSAR data (from Sentinel-1 satellites) all over the European Union. Among the several products available, we used Level-2 calibrated products (datasets: S1D egms_l2b_168_0811_iw2_vv and S1A egms_l2b_015_0261_iw2_vv) that are line-of-sight velocity (V_{LOS}) in ascending and descending orbits referenced to a model derived from global navigation satellite system time-series data. We used some post-processing tools to implement the MT-InSAR data. Firstly, the availability of ascending and descending dataset orbits allowed us to calculate the vertical and east–west components of the velocity using the equation described by Bejar-Pizarro et al. [60]. We used the vertical component of velocity (of Sentinel-1) to implement the velocity of inclinometers that typically measure only the horizontal component. Moreover, to better compare the datasets with different incident angles, we projected the V_{LOS} along the slope using the

C factor [60] based on the slope and aspect derived from SRTM DTM [61]. Finally, we made a sum time series of all datasets to estimate the displacement for the whole period (1992–2020). The periods with data gaps were filled by connecting a linear regression of each time series. The overlapping period (March 2018–June 2020) of Sentinel-1 with ground-based monitoring data allowed for data comparison and cross-validation.

2.2.2. Ground-Based Monitoring

As a result of a project funded by Regione Liguria in the framework of the “2015 Geo hydrological risk mitigation works regional program”, drilling activities were carried out to identify the stratigraphic sequence and to set up a ground-monitoring network. That year, the first geognostic survey was carried out by drilling 4 boreholes with piezometric cases in the village of Arzeno, which showed complex stratigraphy and hydrogeology. Then, in 2016, an extensive geophysical survey was launched to properly plan a second geognostic campaign that was carried out in 2017 by drilling 6 boreholes; among them, 2 were equipped with inclinometer cases and 4 piezometric cases.

In March 2018, thanks to the presence of the described boreholes, the monitoring network was finally set up (Figure 4). In the piezometric cases of Prato di Reppia (PDR) and Arzeno (ARZ), two automatic piezometers were installed. A smart network controlled their logging and data storage. In detail, piezometers log and transmit data to a WiFi modem with the help of additional network nodes linking the sensors to the modem as repeaters. Data loggers store the data even without linkage to the modem; stored data are transmitted as soon as the connection is restored.

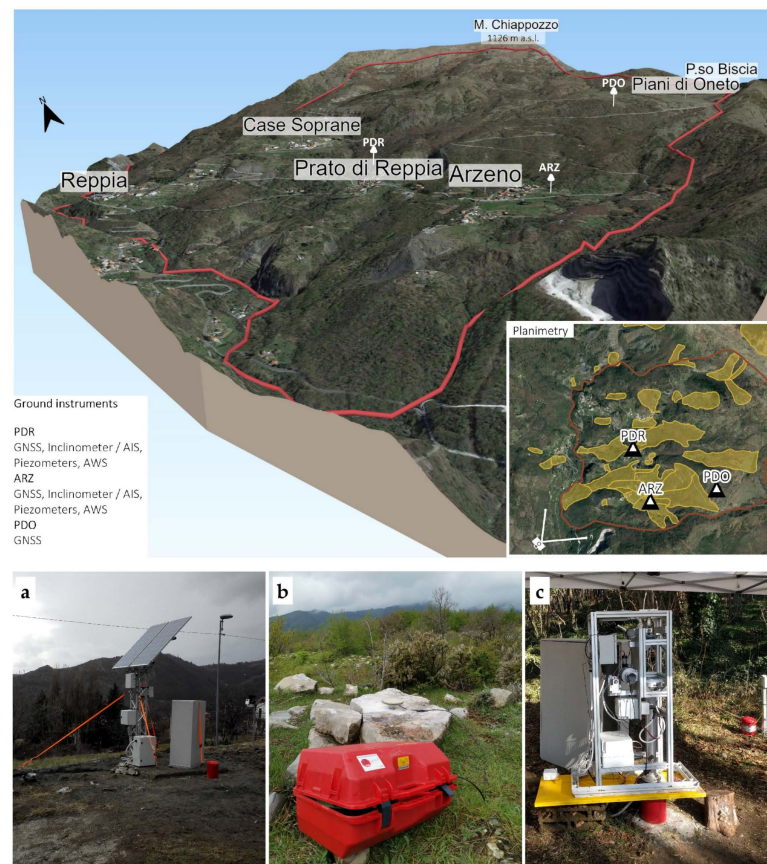


Figure 4. 3D view from SW of in situ monitoring network at sites (a) ARZ; (b) PDO; and (c) PDR.

Moreover, alarms and/or thresholds can be set. In the PDR borehole, quarterly inclinometric measurements [62] were planned, and in the ARZ borehole, an experimental, automatic inclinometric system (AIS) was installed [63]. Measurements were scheduled at a rate of 2 measures/day. Additionally, in ARZ, an automatic weather station (AWS)

was positioned. As a modem link can remotely control AIS, it acts as the primary node of the smart network, collecting data from the piezometers and AWS. To crosscheck deep measurements, a network of GNSS benchmarks was also set up in the two monitoring sites. After one year of monitoring, a third benchmark was placed in the upper sector of the phenomenon, corresponding to a limestone outcrop nearby Piani di Oneto (PDO), to compare the activity of the different sectors. GNSS surveys were carried out contemporarily with the manual inclinometric measurements. Each GNSS survey campaign was executed using a GNSS static high-precision technique with an occupation time variable from 2 to 3 h for each benchmark and with a static epoch acquisition rate of 5 s, using a Leica 1200 GPS/GLONASS. To maximize measurement repeatability, the antenna was directly mounted over a 5/8-inch fillet, cemented on a concrete basement. All baseline calculations were computed, starting from the “GENU” CORS (Continuously Operating Reference Station) belonging to the Ligurian Regional GNSS reference network. Network compensation strategy, calculated using WAYPOINT GRAFNET multi-base software, was performed using precise ephemerides with a least-square-weighted constrained network (weighted fixed confidence interval for GENU of 5 mm standard deviation).

After 20 months of monitoring, the ARZ borehole reached a level of deformation that hampered the inclinometric measurements, which was determined thanks to the load cell alert [64]. Due to the modularity of the AIS, the system was moved and installed in the PDR borehole (Figure 5) to continue high-frequency monitoring for nearly one year before the end of measurements was caused the same deformation issues. Additionally, in PDR, due to the presence of a secondary sliding surface located in the upper sector of the borehole, monitoring was continued in the sector mentioned above to acquire further data before the AIS removal.

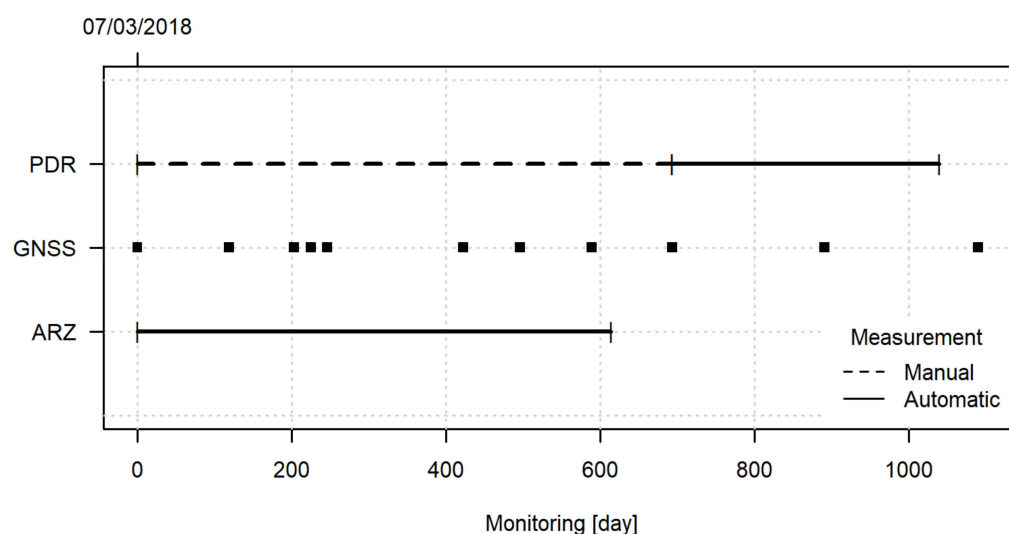


Figure 5. Timeline of ground monitoring.

3. Results

3.1. Multi Platform Satellite Interferometry

Thanks to good density and spatial data distribution, the InSAR analysis allowed us to detect the most active sectors of this large DsGSD. Data from ERS (Figure 6a), Envisat (Figure 6b), CSK (Figure 6c) and Sentinel-1 (Figure 6d) satellites show that the spatial distribution and displacement rate maintained almost the same pattern over the last 28 years (1992–2020). It is possible to observe that the sectors with higher velocity (V_{slope}) are located around the settlement of Arzeno (35–45 mm/yr) and Prato di Reppia hamlet (20–35 mm/yr). Evidence of damage in this area is the reason why the ground monitoring was installed here. A sector with weaker movement (10–20 mm/yr) is located between Arzeno and Piani di Oneto, the depression described before. Another sector with slow

movement is located West of Mt. Chiappozzo. The sector of Case Soprane and Reppia (located over a ridge) is stable, as are the areas outside the deformation.

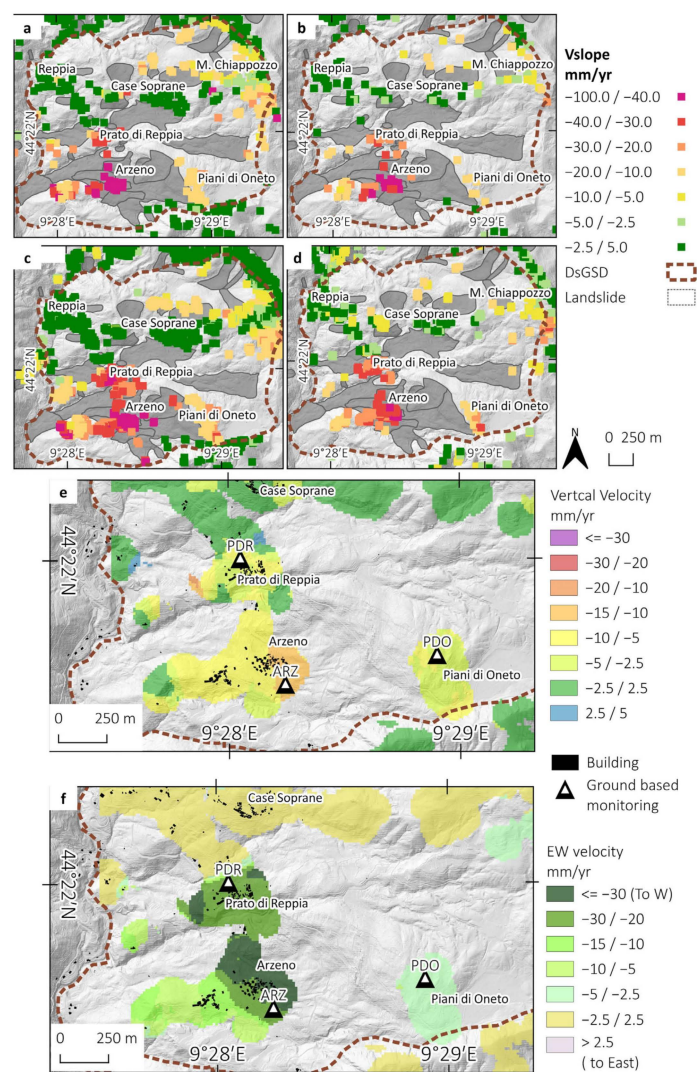


Figure 6. InSAR data results over the Arzeno–Prato study area. Shown is the velocity along the line of sight (V_{LOS}) for the descending geometry of (a) ERS, (b) Envisat, (c) Cosmo-Skymed, (d) Sentinel-1 satellites. With ascending and descending geometries of Sentinel-1, it was possible to resolve the vertical panel (e) and East-West panel (f) components of the velocity.

The availability of ascending and descending geometries allowed us to compute the velocity's east-west (Figure 6f) and vertical (Figure 6e) components. For instance, Sentinel-1 data (2015–2020) show velocities of up to 35 mm/yr towards the west and 15 mm/yr of subsidence in the hamlet of ARZ. In ARZ and PDR sectors, the horizontal component of velocity is predominant and in agreement with the low slope gradient value ($<20^\circ$). The summarised time-series analysis revealed a total cumulated displacement estimated at 1.3 m for ARZ and 0.8 m in PDR over 28 years of monitoring (Figure 7a). The boxplot of V_{slope} distribution for each dataset shows that the velocity for PDR hamlet (Figure 7c) is almost the same (median of 35 mm/yr) throughout 1992–2020. The ENVISAT dataset shows slow velocity compared to other datasets; however, this could also be related to an underestimation of movement, especially acceleration periods, because the time series shows several date gaps in the acquisitions. In the case of ARZ (Figure 7b) ERS shows a higher V_{slope} (55 mm/yr) compared to other datasets (40 mm/yr); however, the low number of PSs (20) compared to other datasets (up to 200 for CSK and Sentinel-

1) may have influenced the velocity distributions. We also analyzed the Sentinel-1 data (2015–2020) available from the European Ground Motion Service—EGMS (<https://egms.land.copernicus.eu/> (accessed on 12 November 2022)) portal. Although they are elaborated at a coarse scale and are therefore less sensitive to trends at the local scale, both the velocity and time series agree with the Sentinel-1 processing supplied by Regione Liguria.

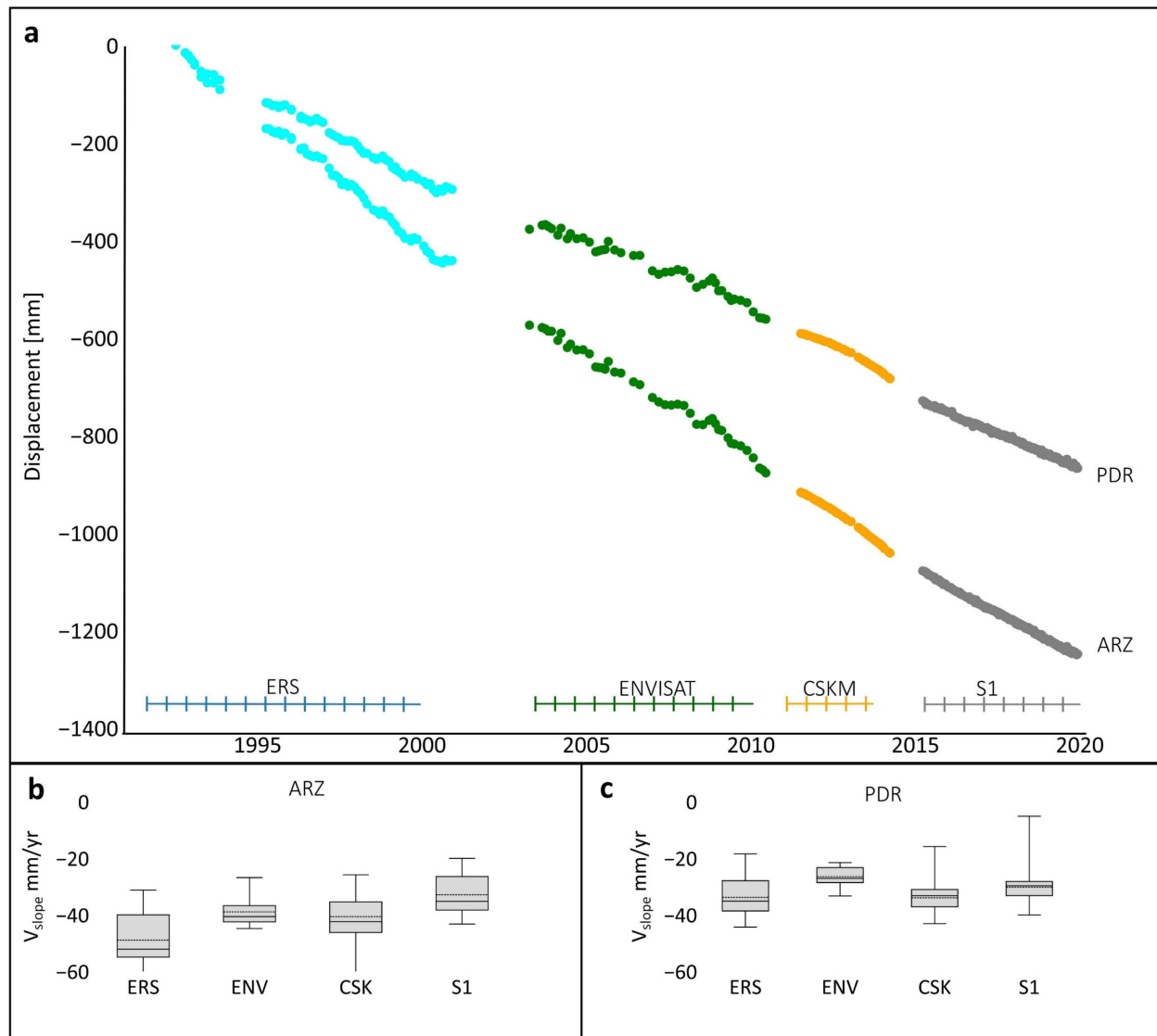


Figure 7. (a) Cumulated Vslope displacement time series (1992–2020) spatially averaged of the PS covering the PDR and ARZ hamlets; (b) Box-plot of Vslope distribution for each satellite dataset used on the ARZ hamlet; (c) Box-plot of Vslope distribution for each satellite dataset used on the PDR hamlet.

3.2. Surface and Sub-Soil Deformations

Piezometers highlighted different behavior between the two cases, as depicted in Figure 8, with different water table responses after rain events. In particular, PDR shows a more rapid increase of ground water level (GWL), up to the surface in some cases, compared to ARZ.

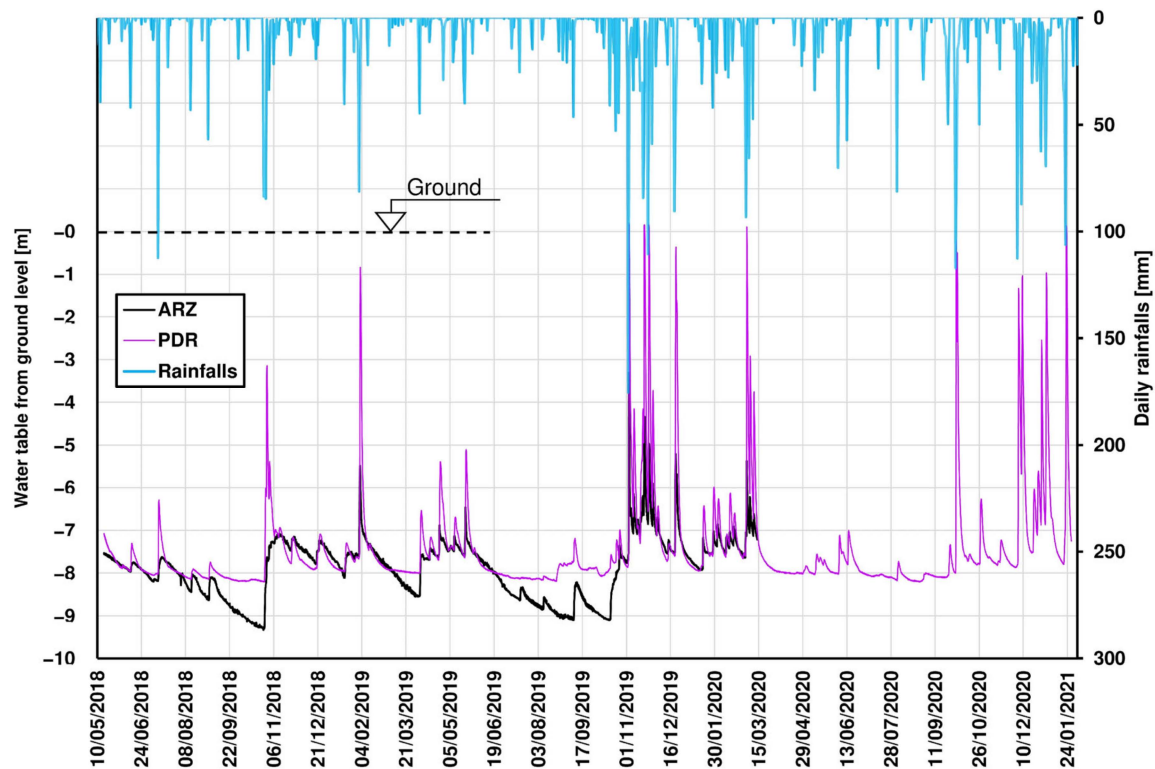


Figure 8. GWL and AWS time series.

Inclinometric measurements provided insights into the two boreholes' sliding surface depth (Figure 9). The main surface of PDR is located at -49 m with a cumulate displacement of 32.2 mm; secondary surfaces are at -22 and -28 m. Both surfaces are located in a fractured ophiolitic breccia. In ARZ, the surface is 17 m deep, at the contact of the landslide deposit with ophiolitic bedrock. Its cumulated displacement was 23.1 mm over the investigated period. Moreover, the high-frequency measurements, provided by the AIS, provided a time series of displacements at selected/noteworthy depths, allowing a better interpretation of the dynamics of the phenomenon.

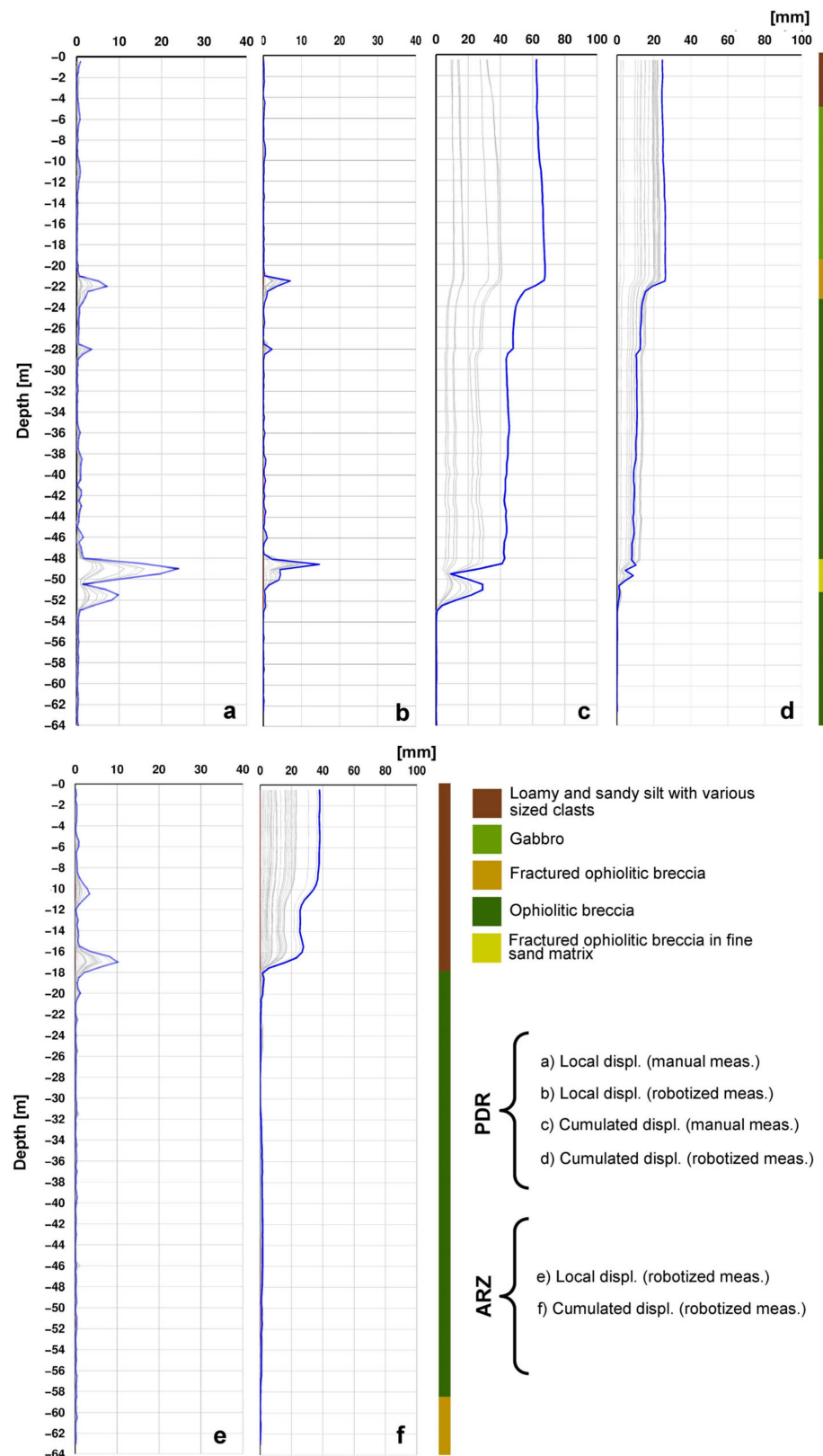


Figure 9. Inclinometric data with simplified stratigraphy (blue line: last measure; grey lines: intermediate measurements; red line—coincident with y axis: first measurement).

4. Discussion

Monitoring large phenomena poses several challenges that need to be adequately managed to obtain reliable data. Firstly, the correct approach should be selected; these phenomena feature slow to very slow displacement rates, so instrumentation with adequate accuracy should be used [24]. In the studied site, the solution that was considered the most effective was to combine InSAR data, which is capable of measuring slow-moving phenomena and is unaffected by cloud cover [64], with adequate in situ instrumentation. Concerning ground measurement, the choice of inclinometric measurements allowed us to obtain, in addition to the overall surficial displacement, the location of the sliding surfaces. Additionally, using the experimental, robotized inclinometer provided high-frequency inclinometric readings, which allowed us to analyze the kinematics of the phenomena over time [40]. GNSS benchmarks were used as a reference for surface displacements with periodic surveys. Finally, the piezometers and AWS were used as proxies of acceleration measured in the shallow sectors, particularly in PDR. The choice of two monitoring sites offered several advantages, such as allowing us to analyze the investigated phenomena in higher detail and, furthermore, characterizing different behavior of the two monitored sites in terms of response time after heavy rainfall events, depth and number of sliding surfaces. These features allowed us to define two different sectors of the DsGSD. By contrast, the availability of only one robotized inclinometer made it necessary to carry out manual measure at the other site, thus complicating the monitoring campaigns' logistics and duration. Nevertheless, the use of AIS helped substantially in the comprehension of the kinematics of the phenomena, as its high-frequency acquisition and remote operability allowed us to check, in near-real-time, the evolution of the deformation in the case of a heavy rainfall event. Regarding the combined use of remote and ground approaches, the monitoring network proved its reliability, as the different methodologies provided comparable results, confirming the validity of the approach. The deep, surface and remote measurements are, in fact, in agreement (e.g., the comparison between PDR inclinometric and GNSS measures provided a regression coefficient $r = 0.98$ with a high significance level $p < 0.001$) in describing the kinematics of the phenomenon. Regarding the piezometric measurements details, the two sites showed a completely different behavior (Figure 8), even though they are only located approximately 700 m apart. During the most intense rain events, these differences tended to decrease, and the monitoring network recorded an increase in the displacement rate. The analysis of the AIS and groundwater data of the PDR site for the period February–July 2020 (Figure 10c) showed that a series of rainfall events at the end of the rainy period caused an increase of GW level up to the artesian state (+0.01 m) (Figure 11c) at the beginning of March. These increases caused a peak acceleration of up to 120 mm/yr (5 mm in 15 days). Later, from April to June 2020, when no noteworthy rainfall (and consequent GW level increase) occurred, the rate of displacement went back to the average values of previous years. This paroxysm event evidences the importance of having daily monitoring by AIS and piezometers: InSAR data underestimated the early March 2020 peak (Figure 10a,b) (possibly a phase unwrapping problem), and GNSS or manual inclinometers have low measure frequency to describe the acceleration period [65] correctly.

The InSAR monitoring showed good agreement with the in-situ monitoring data (Figure 11), allowing about 28 years of displacement measurements. The overlapping measures (April 2018–June 2020) indicate that GNSS, the inclinometers and the InSAR data show a linear trend. The acceleration that affected the PDR sector occurred in the winter of 2019–2020 and was detected by manual inclinometers, AIS and GNSS, while InSAR data seems underestimated the acceleration. In particular, an acceleration in the PDR sector that occurred in March 2020 was detected only by AIS (Figure 11d). It is also possible to appreciate from the AIS of PDR that the displacement rate after April 2020 slowed down to the values detected by InSAR in previous years. InSAR data offers a deformation time series that can effectively track past trends in the study area. This dataset is global and often free, but it requires calibration with on-site observations, and the debate regarding

its interpretation is ongoing. Without ground-truthing, the final results may even present conflicting insights regarding processing approaches [66–68].

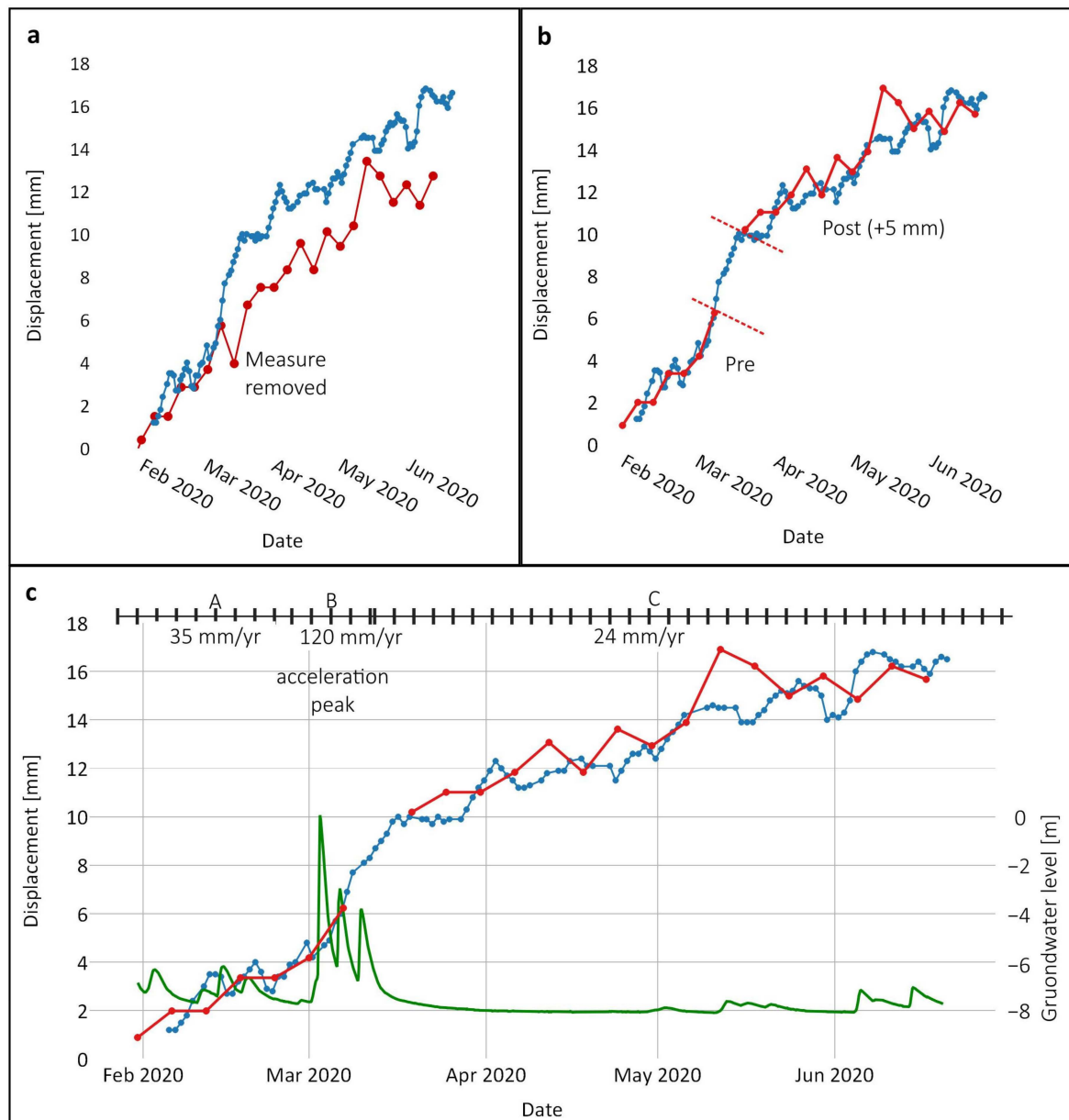


Figure 10. Comparison between AIS displacements (top of the borehole) and InSAR data from Sentinel-1 EGMS for February–July 2020 at the PDR site. (a) Original Sentinel-1 EGMS time series showing underestimation; (b) EGMS time series divided into pre- and post-acceleration events, the post-event time series is shifted by +6 mm; (c) AIS and InSAR time series compared with GWL data.

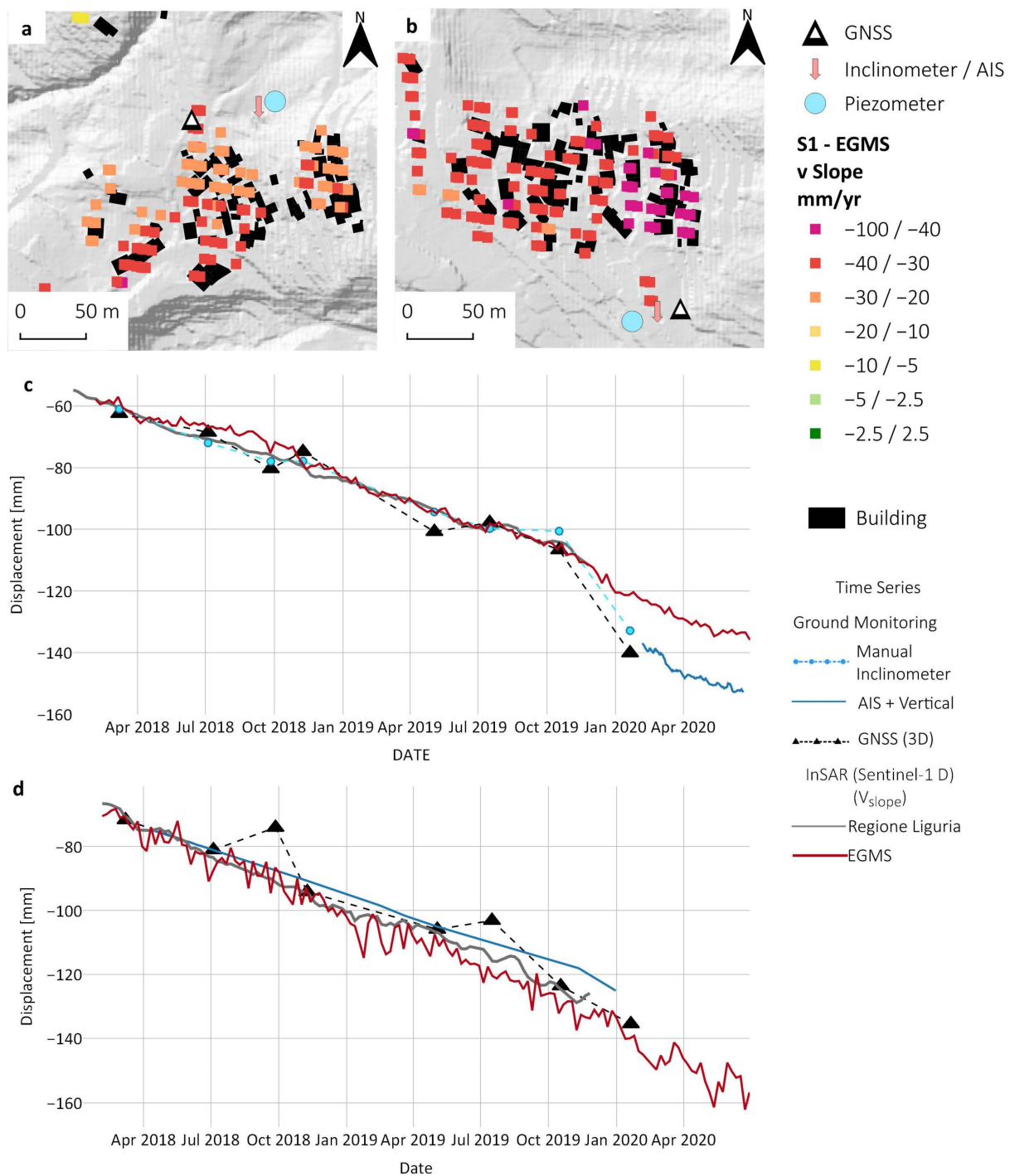


Figure 11. Sentinel-1 V_{slope} data and location of ground instruments for PDR (a) and ARZ (b). Comparison of displacement time series of MT-InSAR of Sentinel-1 (V_{slope} descending dataset), GNSS (3D component) and inclinometers/AIS (with the vertical component from SAR) for the period of overlapping measure (April 2018–June 2020) for the sites PDR (c) and ARZ (d).

Contribution of the Monitoring to Community Safeguard

Concerning the local community, the velocity and the damage detected show that adapting to living on such phenomena could be feasible and affordable with ordinary maintenance of buildings and infrastructure. Moreover, the data acquired in the monitoring campaign and further analyses with the InSAR dataset [52] suggests a revision of the current landslide zonation map for improved land-planning support. In addition, the

SAR data could help to focus mitigation actions on the most critical area [69], improving the community's resilience and reducing its abandonment. Referring to a broader context, depopulation trends in mountainous areas are uninterruptedly growing over time. Without subsidies from the European Union or national/regional governments, marginalization will continue, thus exposing those territories to further abandonment [70,71]. The Italian situation is consistent with the European Union scenario, where the highest concentrations of abandonment-prone areas are located in mountain regions [72]. To assure the survival of those communities, adopting safeguard measures is necessary. To effectively address a range of issues and ensure comprehensive coverage, it is crucial to adopt a multidisciplinary approach that considers socio-economic factors and a deep understanding of landslides and similar phenomena [73]. A strategic plan should be developed to frame the current situation, monitor its evolution in response to existing pressures and evaluate the effectiveness of any mitigation or subsidy measures put in place [74–76]. Fine-scale and high temporal and spatial resolution data are needed to acquire this knowledge. The proposed approach aims to provide a minimal standard of territorial protection to those areas which, due to the previously explained issues, cannot support establishing an extensive monitoring infrastructure, as opposed to mass tourism mountain areas like ski resorts [77–79]. In the latter cases, available financial resources can support intensive spatial and temporal monitoring of the phenomenon. In contrast, the case study described herein, which is representative of most mountain communities in Italy and Europe, demonstrates that the approach as mentioned earlier can address a knowledge gap regarding the recurring issue of landslides in complex mountain environments, as highlighted by previous studies [7,79]. This approach enabled regional and municipal administrators to understand the phenomena sufficiently, enabling them to evaluate the management of villages, their inhabitants and associated issues. The outcomes provided by intensive monitoring allowed the authorities and technicians to discard several unaffordable technical and economic risk-mitigation solutions. For instance, the regional government has withdrawn its initial proposal to realize drainage pits because the design hypotheses were proven wrong due to the sliding surface depth and inadequate drainage capacity.

5. Conclusions

A DsGSD affects a mountain slope in the Liguria Region (Italy). The area has several hamlets in a marginal mountain community, which are endangered by the phenomenon. The slow movement rate and extension required diverse monitoring instruments as well as satellite-borne and in situ data.

Concerning remote sensing, data obtained by multiple platforms allowed us to reconstruct the past 28 years of deformation. Regarding ground-based measurements, the use of the robotized inclinometer, thanks to its high-frequency monitoring, provided a depth assessment of the sliding surfaces, i.e., -49 m in PDR and -17 m in ARZ, and the quantification of cumulated displacements, which total 32.2 mm and 23.1 mm respectively. In PDR, secondary surfaces at -22 and -28 m were also detected. AIS also allowed the detection of a short but remarkable acceleration (5 mm/15 days) after a severe rainfall event and subsequent groundwater level increase, as confirmed by piezometers and AWS.

This study shows the importance of intensive and multidisciplinary monitoring to correctly cope with slow-moving phenomena. The proposed approach can be easily replicated in other mountain contexts. However, it is important to note that InSAR data should be carefully analyzed and interpreted to obtain reliable results, and in situ approaches need meticulous planning, as they are time-consuming, especially during installation and maintenance phases.

Lastly, concerning the community settled in the study area, the result of monitoring, combined with the social and economic assessment, can be used by the authorities and inhabitants to plan the most affordable solution for coexistence with DsGSD. Data are important for the land managers, at all levels, to plan correct mitigation actions in ordinary times and protection measures during emergencies. With the current state of marginality

and abandonment, these actions are the best safeguard for the mountain settlements, allowing the survival of local communities and, thus, preventing or at least reducing the abandonment dynamic. Additionally, this setting deserves particular attention in the current global change scenario, which will progressively worsen the climatic impacts in those areas, making them even more vulnerable to geo-hydrological instabilities.

Author Contributions: Conceptualization, D.G., P.A. and F.F.; data curation, D.G., P.A., D.N. and M.B.; formal analysis, D.G., P.A., D.N. and M.B.; funding acquisition, F.P.; investigation, D.G., P.A., M.B. and F.F.; methodology, D.G., P.A., D.N. and F.F.; project administration, P.A. and F.F.; software, P.A.; supervision, P.A., F.P. and F.F.; validation, M.B.; visualization, D.G. and D.N.; writing—original draft, D.G., D.N. and F.F.; writing—review and editing, P.A., D.N., M.B. and F.P. All authors have read and agreed to the published version of the manuscript.

Funding: This research was funded by Regione Liguria and Ne Municipality.

Data Availability Statement: Data sharing not applicable for ground monitoring data. On the geo-portal of Regione Liguria it is possible to freely download the following data: Landides (IFFI inventories) <https://www.regione.liguria.it/open-data/item/7069-inventario-dei-fenomeni-franosi-sc-1-10000-progetto-iffi.html> (accessed on 3 February 2022); Geological Map 1:25,000: <https://www.regione.liguria.it/open-data/item/7089-carg-carte-geologiche-sc-1-25000-riferite-al-foglio-232-sestri-levante-sc-1-50000.html> (accessed on 3 February 2022); Hydrographic network: <https://www.regione.liguria.it/open-data/item/22430-reticolo-idrografico-e-bacini-idrografici-sc-1-10000-dgr-n-507-2019.html> (accessed on 3 February 2022); The Sentinel-1 data (ascending and descending dataset) for the period 2015–2020 can be downloaded from EGMS—Copernicus service <https://egms.land.copernicus.eu/> (accessed on 3 February 2022).

Acknowledgments: Authors would like to thank Martina Cignetti for her constructive revision of the text helping to substantially improve the paper.

Conflicts of Interest: The authors declare no conflict of interest.

References

- Hungr, O.; Leroueil, S.; Picarelli, L. The Varnes classification of landslide types, an update. *Landslides* **2014**, *11*, 167–194. [\[CrossRef\]](#)
- Galadini, F.; Colini, L.; Giaccio, B.; Messina, P.; Salvi, S.; Sposato, A. Persisting effects of the Colfiorito (Central Italy) Pleistocene paleo-landslide in the planning of land use: Upper palaeolithic and proto-historical coexistence and antique-modern modifications. *Environ. Geol.* **2003**, *43*, 621–634. [\[CrossRef\]](#)
- Benedetti, G.; Bernardi, M.; Bonaga, G.; Borgatti, L.; Continelli, F.; Ghirelli, M.; Guerra, C.; Landuzzi, A.; Lucente, C.C.; Marchi, G. San Leo: Centuries of coexistence with landslides. In *Landslide Science and Practice: Risk Assessment, Management and Mitigation*; Springer: Berlin/Heidelberg, Germany, 2013; Volume 6, pp. 529–537.
- Sallustio, L.; Pettenella, D.; Merlini, P.; Romano, R.; Salvati, L.; Marchetti, M.; Corona, P. Assessing the economic marginality of agricultural lands in Italy to support land use planning. *Land Use Policy* **2018**, *76*, 526–534. [\[CrossRef\]](#)
- Dubois, A.; Sielker, F. Digitalization in sparsely populated areas: Between place-based practices and the smart region agenda. *Reg. Stud.* **2022**, *56*, 1771–1782. [\[CrossRef\]](#)
- Bengtson, V.L. From Ageism to the Longevity Revolution: Robert Butler, Pioneer. *Gerontologist* **2014**, *54*, 1064–1069. [\[CrossRef\]](#)
- Klein, J.A.; Tucker, C.M.; Nolin, A.W.; Hopping, K.A.; Reid, R.S.; Steger, C.; Grêt-Regamey, A.; Lavorel, S.; Müller, B.; Yeh, E.T.; et al. Catalyzing Transformations to Sustainability in the World’s Mountains. *Earth’s Futur.* **2019**, *7*, 547–557. [\[CrossRef\]](#)
- Butler, R.N. Age-ism: Another form of bigotry. *Gerontologist* **1969**, *9*, 243–246. [\[CrossRef\]](#)
- ISTAT. *L’indice di Vulnerabilità Sociale e Materiale*; Istituto Nazionale Di Statistica: Rome, Italy, 2017.
- Mazziotta, M.; Pareto, A. A composite index for measuring Italian regions’ development over time. *Ital. J. Econ. Demogr. Stat. Stud.* **2014**, *68*.
- Giordan, D.; Wrzesniak, A.; Allasia, P. The Importance of a Dedicated Monitoring Solution and Communication Strategy for an Effective Management of Complex Active Landslides in Urbanized Areas. *Sustainability* **2019**, *11*, 946. [\[CrossRef\]](#)
- Cruden, D.; Varnes, D. Landslides: Investigation and mitigation. Chapter 3—Landslide types and processes. *Transp. Res. Board Spec. Rep.* **1996**, *247*.
- Agliardi, F.; Crosta, G.B.; Frattini, P. Slow rock-slope deformation. In *Landslides*; Cambridge University Press: Cambridge, UK, 2013; pp. 207–221.
- Huang, R. Mechanisms of large-scale landslides in China. *Bull. Eng. Geol. Environ.* **2012**, *71*, 161–170. [\[CrossRef\]](#)
- Lacroix, P.; Handwerker, A.L.; Bièvre, G. Life and death of slow-moving landslides. *Nat. Rev. Earth Environ.* **2020**, *1*, 404–419. [\[CrossRef\]](#)

16. Timilsina, M.; Bhandary, N.P.; Dahal, R.K.; Yatabe, R. Distribution probability of large-scale landslides in central Nepal. *Geomorphology* **2014**, *226*, 236–248. [[CrossRef](#)]
17. Dramis, F.; Sorriso-Valvo, M. Deep-seated gravitational slope deformations, related landslides and tectonics. *Eng. Geol.* **1994**, *38*, 231–243. [[CrossRef](#)]
18. Pánek, T.; Klimeš, J. Temporal behavior of deep-seated gravitational slope deformations: A review. *Earth-Sci. Rev.* **2016**, *156*, 14–38. [[CrossRef](#)]
19. Lan, H.; Liu, X.; Li, L.; Li, Q.; Tian, N.; Peng, J. Remote Sensing Precursors Analysis for Giant Landslides. *Remote Sens.* **2022**, *14*, 4399. [[CrossRef](#)]
20. Frattini, P.; Crosta, G.B.; Rossini, M.; Allievi, J. Activity and kinematic behaviour of deep-seated landslides from PS-InSAR displacement rate measurements. *Landslides* **2018**, *15*, 1053–1070. [[CrossRef](#)]
21. Cignetti, M.; Godone, D.; Zucca, F.; Bertolo, D.; Giordan, D. Impact of Deep-seated Gravitational Slope Deformation on urban areas and large infrastructures in the Italian Western Alps. *Sci. Total Environ.* **2020**, *740*, 140360. [[CrossRef](#)]
22. Frattini, P.; Crosta, G.B.; Allievi, J. Damage to buildings in large slope rock instabilities monitored with the PSInSARTM technique. *Remote Sens.* **2013**, *5*, 4753–4773. [[CrossRef](#)]
23. Cignetti, M.; Godone, D.; Wrzesniak, A.; Giordan, D. Structure from motion multisource application for landslide characterization and monitoring: The Champelas du Col case study, Sestriere, north-western Italy. *Sensors* **2019**, *19*, 2364. [[CrossRef](#)] [[PubMed](#)]
24. Chae, B.G.; Park, H.J.; Catani, F.; Simoni, A.; Berti, M. Landslide prediction, monitoring and early warning: A concise review of state-of-the-art. *Geosci. J.* **2017**, *21*, 1033–1070. [[CrossRef](#)]
25. Bagwari, S.; Gehlot, A.; Singh, R.; Priyadarshi, N.; Khan, B. Low-Cost Sensor-Based and LoRaWAN Opportunities for Landslide Monitoring Systems on IoT Platform: A Review. *IEEE Access* **2022**, *10*, 7107–7127. [[CrossRef](#)]
26. Le Breton, M.; Bontemps, N.; Guillemot, A.; Baillet, L.; Larose, É. Landslide monitoring using seismic ambient noise correlation: Challenges and applications. *Earth Sci. Rev.* **2021**, *216*, 103518. [[CrossRef](#)]
27. Thirugnanam, H.; Uhlemann, S.; Reghunadh, R.; Ramesh, M.V.; Rangan, V.P. Review of Landslide Monitoring Techniques with IoT Integration Opportunities. *IEEE J. Sel. Top. Appl. Earth Obs. Remote Sens.* **2022**, *15*, 5317–5338. [[CrossRef](#)]
28. Casagli, N.; Frodella, W.; Morelli, S.; Tofani, V.; Ciampalini, A.; Intrieri, E.; Raspini, F.; Rossi, G.; Tanteri, L.; Lu, P. Spaceborne, UAV and ground-based remote sensing techniques for landslide mapping, monitoring and early warning. *Geoenvironmental Disasters* **2017**, *4*, 1–23. [[CrossRef](#)]
29. Notti, D.; Wrzesniak, A.; Dematteis, N.; Lollino, P.; Fazio, N.L.; Zucca, F.; Giordan, D. A multidisciplinary investigation of deep-seated landslide reactivation triggered by an extreme rainfall event: A case study of the Monesi di Mendatica landslide, Ligurian Alps. *Landslides* **2021**, *18*, 2341–2365. [[CrossRef](#)]
30. Chen, R.-F.; Lee, C.-Y.; Yin, H.-Y.; Huang, H.-Y.; Cheng, K.-P.; Lin, C.-W. Monitoring the Deep-Seated Landslides by Using ALOS/PALSAR Satellite Imagery in the Disaster Area of 2009 Typhoon Morakot, Taiwan. In *Advancing Culture of Living with Landslides*; Springer: Cham, Switzerland, 2017; pp. 239–247.
31. Crippa, C.; Agliardi, F.; Spreafico, M.C.; Frattini, P.; Crosta, G.B.; Valbuzzi, E. Semi-automated regional analysis of slow-moving landslide activity and kinematics using PS-InSAR data. In *Geophysical Research Abstracts*; Springer: Cham, Switzerland, 2019; Volume 21.
32. Cignetti, M.; Godone, D.; Notti, D.; Zucca, F.; Meisina, C.; Bordoni, M.; Pedretti, L.; Lanteri, L.; Bertolo, D.; Giordan, D. Damage to anthropic elements estimation due to large slope instabilities through multi-temporal A-DInSAR analysis. *Nat. Hazards* **2022**, *115*, 1–30. [[CrossRef](#)]
33. Hu, X.; Lu, Z.; Pierson, T.C.; Kramer, R.; George, D.L. Combining InSAR and GPS to Determine Transient Movement and Thickness of a Seasonally Active Low-Gradient Translational Landslide. *Geophys. Res. Lett.* **2018**, *45*, 1453–1462. [[CrossRef](#)]
34. Godone, D.; Allasia, P.; Borrelli, L.; Gullà, G. UAV and structure from motion approach to monitor the Maierato landslide evolution. *Remote Sens.* **2020**, *12*, 1039. [[CrossRef](#)]
35. Kaneda, H.; Kono, T. Discovery, Controls, and Hazards of Widespread Deep-Seated Gravitational Slope Deformation in the Etsumi Mountains, Central Japan. *J. Geophys. Res. Earth Surf.* **2017**, *122*, 2370–2391. [[CrossRef](#)]
36. Allasia, P.; Baldo, M.; Giordan, D.; Godone, D.; Wrzesniak, A.; Lollino, G. Near Real Time Monitoring Systems and Periodic Surveys Using a Multi Sensors UAV: The Case of Ponzano Landslide. In *IAEG/AEG Annual Meeting Proceedings, San Francisco, California, 2018—Volume 1*; Springer International Publishing: Cham, Switzerland, 2018; pp. 303–310.
37. Barla, G.; Antolini, F.; Barla, M.; Mensi, E.; Piovano, G. Monitoring of the Beauregard landslide (Aosta Valley, Italy) using advanced and conventional techniques. *Eng. Geol.* **2010**, *116*, 218–235. [[CrossRef](#)]
38. Dematteis, N.; Wrzesniak, A.; Allasia, P.; Bertolo, D.; Giordan, D. Integration of robotic total station and digital image correlation to assess the three-dimensional surface kinematics of a landslide. *Eng. Geol.* **2022**, *303*, 106655. [[CrossRef](#)]
39. Uhlemann, S.; Smith, A.; Chambers, J.; Dixon, N.; Dijkstra, T.; Haslam, E.; Meldrum, P.; Merritt, A.; Gunn, D.; Mackay, J. Assessment of ground-based monitoring techniques applied to landslide investigations. *Geomorphology* **2016**, *253*, 438–451. [[CrossRef](#)]
40. Allasia, P.; Godone, D.; Giordan, D.; Guenzi, D.; Lollino, G. Advances on measuring deep-seated ground deformations using robotized inclinometer system. *Sensors* **2020**, *20*, 3769. [[CrossRef](#)] [[PubMed](#)]
41. Salvati, P.; Petrucci, O.; Rossi, M.; Bianchi, C.; Pasqua, A.A.; Guzzetti, F. Gender, age and circumstances analysis of flood and landslide fatalities in Italy. *Sci. Total Environ.* **2018**, *610–611*, 867–879. [[CrossRef](#)] [[PubMed](#)]

42. Roccati, A.; Faccini, F.; Luino, F.; Turconi, L.; Guzzetti, F. Rainfall events with shallow landslides in the Entella catchment, Liguria, northern Italy. *Nat. Hazards Earth Syst. Sci.* **2018**, *18*, 2367–2386. [[CrossRef](#)]
43. Trigila, A.; Iadanza, C.; Spizzichino, D. Quality assessment of the Italian Landslide Inventory using GIS processing. *Landslides* **2010**, *7*, 455–470. [[CrossRef](#)]
44. Brandolini, P.; Canepa, G.; Faccini, F.; Robbiano, A.; Terranova, R. Geomorphological and geo-environmental features of the Graveglia Valley (Ligurian Apennines, Italy). *Geogr. Fis. e Din. Quat.* **2007**, *30*, 99–116.
45. Bortolotti, V.; Principi, G.; Abbate, E.; Chiari, M.; Aiello, I.W.; Mannori, G.; Pandeli, E. Carta Geologica d'Italia alla scala 1: 50.000, Foglio 232 Sestri Levante. *Serv. Geol. D'Italia Roma* **2011**.
46. Capponi, G.; Crispini, L.; Federico, L.; Malatesta, C. Geology of the eastern ligurian alps: A review of the tectonic units. *Ital. J. Geosci.* **2016**, *135*, 157–169. [[CrossRef](#)]
47. Franceschini, R.; Rosi, A.; Del Soldato, M.; Catani, F.; Casagli, N. Integrating multiple information sources for landslide hazard assessment: The case of Italy. *Sci. Rep.* **2022**, *12*, 20724. [[CrossRef](#)]
48. Guzzetti, F. Landslide fatalities and the evaluation of landslide risk in Italy. *Eng. Geol.* **2000**, *58*, 89–107. [[CrossRef](#)]
49. Guzzetti, F.; Stark, C.P.; Salvati, P. Evaluation of flood and landslide risk to the population of Italy. *Environ. Manag.* **2005**, *36*, 15–36. [[CrossRef](#)] [[PubMed](#)]
50. Salvati, P.; Bianchi, C.; Rossi, M.; Guzzetti, F. Societal landslide and flood risk in Italy. *Nat. Hazards Earth Syst. Sci.* **2010**, *10*, 465–483. [[CrossRef](#)]
51. Bortolotti, V.; Principi, G. The Bargonasco—Upper Val Graveglia ophiolitic succession, northern apennines, Italy. *Ofioliti* **2003**, *28*, 137–140. [[CrossRef](#)]
52. Balbi, E.; Ferretti, G.; Ferrando, A.; Faccini, F.; Crispini, L.; Cianfarra, P.; Scafidi, D.; Barani, S.; Tosi, S.; Terrone, M. CAPS: A New Method for the Identification of Different Surface Displacements in Landslide and Subsidence Environments through Correlation Analysis on Persistent Scatterers Time-Series from PSI. *Remote Sens.* **2022**, *14*, 3791. [[CrossRef](#)]
53. Sacchini, A.; Faccini, F.; Ferraris, F.; Firpo, M.; Angelini, S. Large-scale landslide and deep-seated gravitational slope deformation of the Upper Scrivia Valley (Northern Apennine, Italy). *J. Maps* **2016**, *12*, 344–358. [[CrossRef](#)]
54. Di Martire, D.; Paci, M.; Confuorto, P.; Costabile, S.; Guastaferro, F.; Verta, A.; Calcaterra, D. A nation-wide system for landslide mapping and risk management in Italy: The second Not-ordinary Plan of Environmental Remote Sensing. *Int. J. Appl. Earth Obs. Geoinf.* **2017**, *63*, 143–157. [[CrossRef](#)]
55. Ferretti, A.; Prati, C.; Rocca, F. Permanent scatterers in SAR interferometry. *IEEE Trans. Geosci. Remote Sens.* **2001**, *39*, 8–20. [[CrossRef](#)]
56. Ferretti, A.; Fumagalli, A.; Novali, F.; Prati, C.; Rocca, F.; Rucci, A. A new algorithm for processing interferometric data-stacks: SqueeSAR. *IEEE Trans. Geosci. Remote Sens.* **2011**, *49*, 3460–3470. [[CrossRef](#)]
57. Crosetto, M.; Solari, L.; Balasis-Levinsen, J.; Bateson, L.; Casagli, N.; Frei, M.; Oyen, A.; Moldestad, D.A.; Mróz, M. Deformation monitoring at european scale: The Copernicus ground motion service. In *Proceedings of the International Archives of the Photogrammetry, Remote Sensing and Spatial Information Sciences—ISPRS Archives; Copernicus GmbH: Göttingen, Germany, 2021; Volume 43*, pp. 141–146.
58. Crosetto, M.; Solari, L.; Mróz, M.; Balasis-Levinsen, J.; Casagli, N.; Frei, M.; Oyen, A.; Moldestad, D.A.; Bateson, L.; Guerrieri, L.; et al. The evolution of wide-area DInSAR: From regional and national services to the European ground motion service. *Remote Sens.* **2020**, *12*, 2043. [[CrossRef](#)]
59. Proietti, S.; Steen Andersen, H. *End-to-End Implementation and Operation of the European Ground Motion Service (EGMS); Copernicus GmbH: Göttingen, Germany, 2021*.
60. Béjar-Pizarro, M.; Notti, D.; Mateos, R.M.; Ezquerro, P.; Centolanza, G.; Herrera, G.; Bru, G.; Sanabria, M.; Solari, L.; Duro, J.; et al. Mapping Vulnerable Urban Areas Affected by Slow-Moving Landslides Using Sentinel-1 InSAR Data. *Remote Sens.* **2017**, *9*, 876. [[CrossRef](#)]
61. Farr, T.G.; Rosen, P.A.; Caro, E.; Crippen, R.; Duren, R.; Hensley, S.; Kobrick, M.; Paller, M.; Rodriguez, E.; Roth, L.; et al. The shuttle radar topography mission. *Rev. Geophys.* **2007**, *45*, 1–33. [[CrossRef](#)]
62. Stark, T.D.; Choi, H. Slope inclinometers for landslides. *Landslides* **2008**, *5*, 339–350. [[CrossRef](#)]
63. Allasia, P.; Lollino, G.; Godone, D.; Giordan, D. Deep displacements measured with a robotized inclinometer system. In *Proceedings of the 10th International Symposium on Field Measurements in Geomechanics—FMGM2018, Rio De Janeiro, Brazil, 16–20 July 2018*.
64. Burrows, K.; Walters, R.J.; Milledge, D.; Spaans, K.; Densmore, A.L. A new method for large-scale landslide classification from satellite radar. *Remote Sens.* **2019**, *11*, 237. [[CrossRef](#)]
65. Herrera, G.; López-Davalillo, J.C.G.; Fernández-Merodo, J.A.; Béjar-Pizarro, M.; Allasia, P.; Lollino, P.; Lollino, G.; Guzzetti, F.; Álvarez-Fernández, M.I.; Manconi, A.; et al. The Differential Slow Moving Dynamic of a Complex Landslide: Multi-sensor Monitoring. In *Advancing Culture of Living with Landslides*; Springer: Cham, Switzerland, 2017; pp. 219–225.
66. Milillo, P.; Giardina, G.; Perissin, D.; Milillo, G.; Coletta, A.; Terranova, C.; Lanari, R. Comment on “pre-collapse space geodetic observations of critical infrastructure: The Morandi bridge, Genoa, Italy” by Milillo et al. (2019). *Remote Sens.* **2020**, *12*, 4016. [[CrossRef](#)]

67. Lanari, R.; Reale, D.; Bonano, M.; Verde, S.; Muhammad, Y.; Fornaro, G.; Casu, F.; Manunta, M. Comment on “Pre-Collapse Space Geodetic Observations of Critical Infrastructure: The Morandi Bridge, Genoa, Italy” by Milillo et al. (2019). *Remote Sens.* **2020**, *12*, 4011. [[CrossRef](#)]
68. Milillo, P.; Giardina, G.; Perissin, D.; Milillo, G.; Coletta, A.; Terranova, C. Pre-collapse space geodetic observations of critical infrastructure: The Morandi Bridge, Genoa, Italy. *Remote Sens.* **2019**, *11*, 1403. [[CrossRef](#)]
69. Peduto, D.; Ferlisi, S.; Nicodemo, G.; Reale, D.; Pisciotta, G.; Gullà, G. Empirical fragility and vulnerability curves for buildings exposed to slow-moving landslides at medium and large scales. *Landslides* **2017**, *14*, 1993–2007. [[CrossRef](#)]
70. Godone, D.; Garbarino, M.; Sibona, E.; Garnero, G.; Godone, F. Progressive fragmentation of a traditional Mediterranean landscape by hazelnut plantations: The impact of CAP over time in the Langhe region (NW Italy). *Land Use Policy* **2014**, *36*, 259–266. [[CrossRef](#)]
71. Dax, T.; Schroll, K.; Machold, I.; Derszniak-Noirjean, M.; Schuh, B.; Gaupp-Berghausen, M. Land abandonment in mountain areas of the EU: An inevitable side effect of farming modernization and neglected threat to sustainable land use. *Land* **2021**, *10*, 591. [[CrossRef](#)]
72. Perpiña Castillo, C.; Kavalov, B.; Diogo, V.; Jacobs-Crisioni, C.; Batista e Silvia, F.; Lavalle, C. Agricultural land abandonment in the EU within 2015–2030. *JRC113718 Eur. Comm.* **2018**.
73. Supper, R.; Römer, A.; Jochum, B.; Bieber, G.; Jaritz, W. A complex geo-scientific strategy for landslide hazard mitigation—From airborne mapping to ground monitoring. *Adv. Geosci.* **2008**, *14*, 195–200. [[CrossRef](#)]
74. Mertens, K.; Jacobs, L.; Maes, J.; Poesen, J.; Kervyn, M.; Vranken, L. Disaster risk reduction among households exposed to landslide hazard: A crucial role for self-efficacy? *Land Use Policy* **2018**, *75*, 77–91. [[CrossRef](#)]
75. Thanapackiam, P.; Salleh, K.O.; Ab Ghaffar, F. Vulnerability and adaptation of urban dwellers in slope failure threats—A preliminary observation for the Klang Valley Region. *J. Environ. Biol.* **2012**, *33*, 373–379. [[CrossRef](#)]
76. Murillo-García, F.G.; Rossi, M.; Ardizzone, F.; Fiorucci, F.; Alcántara-Ayala, I. Hazard and population vulnerability analysis: A step towards landslide risk assessment. *J. Mt. Sci.* **2017**, *14*, 1241–1261. [[CrossRef](#)]
77. Giordan, D.; Manconi, A.; Allasia, P.; Bertolo, D. Brief Communication: On the rapid and efficient monitoring results dissemination in landslide emergency scenarios: The Mont de la Saxe case study. *Nat. Hazards Earth Syst. Sci.* **2015**, *15*, 2009–2017. [[CrossRef](#)]
78. Martinotti, G.; Giordan, D.; Giardino, M.; Ratto, S. Controlling factors for deep-seated gravitational slope deformation (DSGSD) in the Aosta Valley (NW Alps, Italy). *Geol. Soc. Spec. Publ.* **2011**, *351*, 113–131. [[CrossRef](#)]
79. Shahgedanova, M.; Adler, C.; Gebrekirstos, A.; Grau, H.R.; Huggel, C.; Marchant, R.; Pepin, N.; Vanacker, V.; Viviroli, D.; Vuille, M. Mountain Observatories: Status and Prospects for Enhancing and Connecting a Global Community. *Mt. Res. Dev.* **2021**, *41*, A1–A15. [[CrossRef](#)]

Disclaimer/Publisher’s Note: The statements, opinions and data contained in all publications are solely those of the individual author(s) and contributor(s) and not of MDPI and/or the editor(s). MDPI and/or the editor(s) disclaim responsibility for any injury to people or property resulting from any ideas, methods, instructions or products referred to in the content.